A model for the dynamics of charging photoreceptor and ionic wind by positive DC corona discharge in Electrophotography

Masato Kobayashi, Norio Uchida and Hidekazu Nogami; Brother Industries, Ltd., Nagoya, Japan

Abstract

To design faster and safer printers with scorotron, it should be highly effective in charging of rotating optical photoconductor (OPC). In high speed printings, the time scale of rotation and charging competes and the charging processes goes to transitional. So, we have to understand dynamics of charging processes for effective charging scorotron. But, the dynamics of charging of rotating OPC by scorotron is not well understood. The authors have recently developed a numerical model of the dynamics of charging rotating OPC and ionic wind by positive DC scorotron. The calculation by the model well reproduced the measured electrostatic potential on rotating OPC and velocity of ionic wind in steady state. The authors show how electrostatic potential on rotating OPC and charge density distribution change with time. The authors also show that the charging time scale by the model.

Introduction

Highly effective charging positive DC scorotron is needed in high speed printing. Staying time of OPC under scorotron decreases with increase of printing speed, the charging time decreases in high speed printing. Addition to this, in the corona plasma region near wire of scorotron, ozone is produced by chemical reactions [1] and transported through ionic wind[2] [3] [4] [5] [6]. Corona current produced by scorotron should be as small as possible, because the production speed of ozone depends linearly on corona current[1]. In high speed printing, the charging processes will be transitional. For effective charging in high speed printing, it is very important to understand the dynamics of charging rotating OPC. Evaluating the time dependence of current and potential on rotating OPC, charging speed and its dependence on corona current will be effective in designing scorotrons. But the dynamics of charging processes are not easy to measure, because time scale of charging is so small.

The numerical simulation is a candidate tool to directly evaluate dynamics of charging on rotating/non-rotating OPC. Though numerical models of potential on rotating OPC surfaces charged by negative corotron and scorotron are proposed in [2] [3] [4] [5] [6], they are formulated in steady state, so charging speed cannot be evaluated. The time dependence of electrostatic potential on OPC surface is modeled by Schaffert, but the model needs two experimental parameters[7].

In **Theory**, the authors show a dynamical model of charging on rotating/non-rotating OPC and the ionic wind. In **Validation**, the authors compare calculated and experimental electric potential of rotating OPC and ionic wind for validation of the model. In **Results and discussion**, the authors show time dependence of potential near scorotron and on OPC, charge density distribution by numerical simulation. The authors derive charging speed from time dependence of calculated potential on non-rotating OPC by fitting. In **Conclusion**, the authors summarize the results.

Theory

The authors model the charging dynamics of rotating OPC in three steps (fig.(1)). In the first step, near the wire, the positive ions are produced in corona plasma region. In the second step, the positive ions are transported to surface of OPC by electric field and airflow. In the third step, the positive ions accumulate on the surface of rotating OPC.

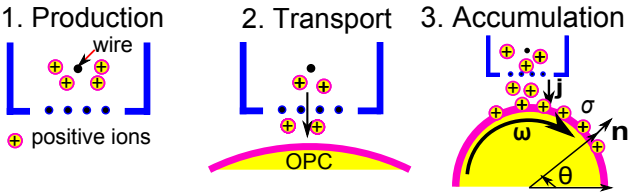

Figure 1. *Schematics of the charging dynamics*

In the first step, the authors model the production of positive ions as the electric current source existing on the wire surface. The distribution of positive ions is described as volumetric charge density. Charge density on the wire ρ_0 is written as follows,

$$\rho_0 = \frac{I}{2\pi a \ell k E_0}, \tag{1}$$

where I, a, ℓ, k, E_0 are corona current, radius and length of wire, mobility of positive ions and the electric field strength on the wire surface respectively. In eq.(1), the authors assumed the charge density is uniform around the surface of the wire. Sarma's assumption[8] is used for E_0, which is kept constant during discharge. E_0 is described by the Peek's law [1] [9],

$$E_0 = 3 \times 10^6 e \left(\delta + 0.03 \sqrt{\frac{\delta}{a}} \right) (\mathrm{V/m}), \tag{2}$$

where e is surface roughness and radius of the wire, and δ is relative density of air. Throughout this paper, the authors set $\delta = 1$.

In the second step, the authors model transfer of positive ions as flow of volumetric charge density, driven by the electric field and air flow. The electric field in the scorotron, between OPC and the grid of scorotron is described as Poisson equation,

$$\nabla \cdot (\varepsilon_0 \nabla \phi) = -\rho, \tag{3}$$

where $\varepsilon_0 = 8.85 \times 10^{-12} \mathrm{A^2 s^4 / (kgm^3)}, \phi, \rho$ is electric permittivity of vacuum, electrostatic potential and volumetric charge density. The flow of charge density is described as equation of charge

conservation,

$$\frac{\partial \rho}{\partial t} + \nabla \cdot \mathbf{J} = 0, \tag{4}$$

$$\mathbf{J} = \rho(-k\nabla\phi + \mathbf{U}), \tag{5}$$

where $\mathbf{J}, \mathbf{U}$ is the current density and the velocity of ionic wind respectively. The dynamics of ionic wind is described by Navier-Stokes equation,

$$\frac{\partial \mathbf{U}}{\partial t} + \mathbf{U}\cdot\nabla\mathbf{U} = -\nu\nabla^2\mathbf{U} - \nabla p_k - \frac{\rho\nabla\phi}{\rho_{air}}, \tag{6}$$

where p_k, ν, ρ_{air} is kinematic pressure, kinematic viscosity and density of air respectively.

In the third step, the authors model the dynamics of charge accumulation on surface of rotating OPC as follows,

$$\frac{\partial \sigma}{\partial t} + (\omega \times \mathbf{r})\cdot\nabla\sigma = -\mathbf{J}\cdot\mathbf{n}, \tag{7}$$

where $\sigma, \omega, \mathbf{r}, \mathbf{n}$ is surface charge on OPC, angular velocity vector of OPC, position vector from center of OPC to its surface and the normal vector on the surface of OPC. In eq.(7), the authors ignored the leak current. In cylindrical coordinate frame with origin located at the center of OPC, eq.(7) can be rewritten as follows,

$$\frac{\partial \sigma}{\partial t} + \omega\frac{\partial \sigma}{\partial \theta} = -\mathbf{J}\cdot\mathbf{n}, \tag{8}$$

where θ is the azimuthal angle(drawn at 3 in fig.(1)). In non-rotating case $\omega = 0$, eq.(8) reduces to

$$\frac{\partial \sigma}{\partial t} = -\mathbf{J}\cdot\mathbf{n}. \tag{9}$$

Assuming OPC as capacitor, electrostatic potential on OPC $V_{opc}(\theta)$ is written as follows,

$$V_{opc}(\theta) = \frac{\varepsilon_r\varepsilon_0\sigma}{d_{opc}}, \tag{10}$$

where ε_r, d_{opc} is relative electric permittivity and the thickness of photosensitive layer. The V_{opc} is used as boundary condition for solving Poisson eq.(3). The authors implemente the model as numerical simulation program, using source codes of OpenFOAM®, the open source CFD toolkit[10]. Throughout this paper, the authors use the physical parameters as listed in tab.(1).

Table 1:Physical parameters

Mobility of positive ions	$k = 1.6\times10^{-4}\mathrm{m}^2/(\mathrm{V}\cdot\mathrm{s})$
Roughness of wire surface	$e = 0.65$
Radius of wire	$a = 60(\mu\mathrm{m})$
Voltage of Grids	$V_G = 700(\mathrm{V})$
Thickness of photosensitive layer	$d_{opc} = 30(\mu\mathrm{m})$
Relative permittivity of photosensitive layer	$\varepsilon_r = 3$
Kinematic viscosity of air	$\nu = 1.55\times10^{-5}\mathrm{m}^2/\mathrm{s}$
Density of air	$\rho_{air} = 1.185(\mathrm{kg}/\mathrm{m}^3)$

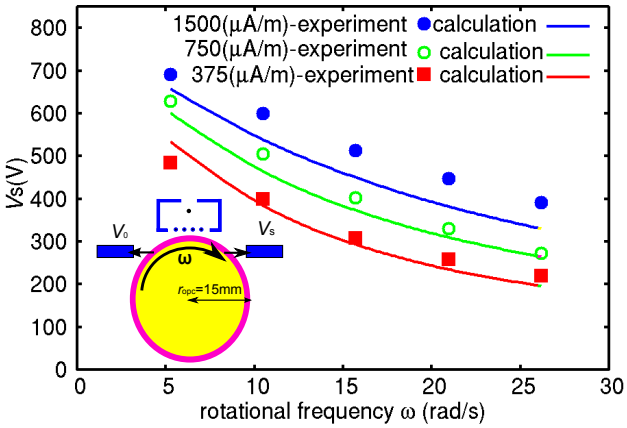

Figure 2. *Experimental and calculated potential on rotating OPC.*

Validation

To validate our model of charging, the authors compare the corona current dependence of calculated and measured potential of rotating OPC after charging. In experiment, the authors measured potential on OPC after charging (denoting it as V_s) with corona current $I/\ell = 375, 750, 1500(\mu\mathrm{A/m})$. The sketch of experiment is drawn on left bottom of fig.(2). In simulation, the authors take the solution of eq.(10) in steady state with the angle $\theta = 30(\mathrm{deg})$ (there located detector) as calculated V_s. The authors take the solution at $t = 0.2(\mathrm{s})$ as steady state in practice. We see the calculation well reproduce the angular velocity dependence and corona current dependence of measured V_s. This indicates that our model well describes steady state of OPC charging.

To validate our model of ionic wind, the authors compare the corona current dependence of calculated and measured velocity of the ionic wind at sampling point of 1mm above the wire (see fig.(3)). In experiment, the authors measured velocity field of ionic wind by particle image velocimetry. The authors draw the velocity $|\mathbf{U}|$ of the solution at time $t = 0.2(\mathrm{s})$ when the flow of ionic wind is in stationary state. We see that the measured corona current dependence of velocity is well reproduced by calculation (fig.(3)).

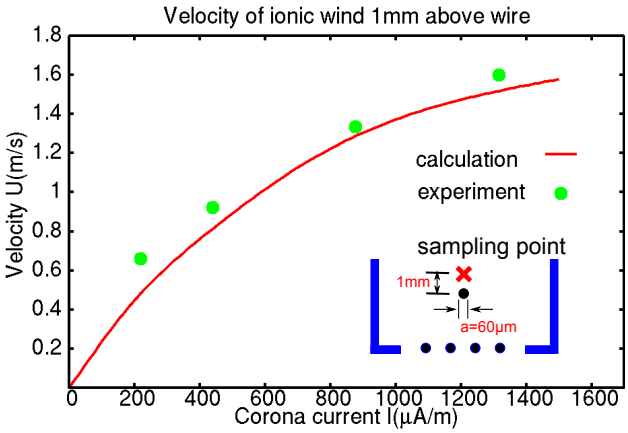

Figure 3. *Experimental and calculated velocity of ionic wind 1mm above wire.*

Results and discussion

The authors discuss the time dependence of calculated electric potential, potential on rotating/non-rotating OPC and charge density with corona current $I/\ell = 375, 750, 1500(\mu\text{A/m})$. In fig.(4), the electric potential contours are drawn in the case with corona current $I/\ell = 1500(\mu\text{A/m})$. In non-rotating OPC($\omega = 0$(rad/s)), the potential between grid and OPC evolves symmetrically with the wire of scorotron. In rotating OPC($\omega = 10.47, 20.94$(rad/s)), the potential on OPC downward of rotation evolves with time and upward doesn't. This results in asymetric shape of potential contour. The asymmetry is larger in slower rotation($\omega = 10.47$(rad/s)).

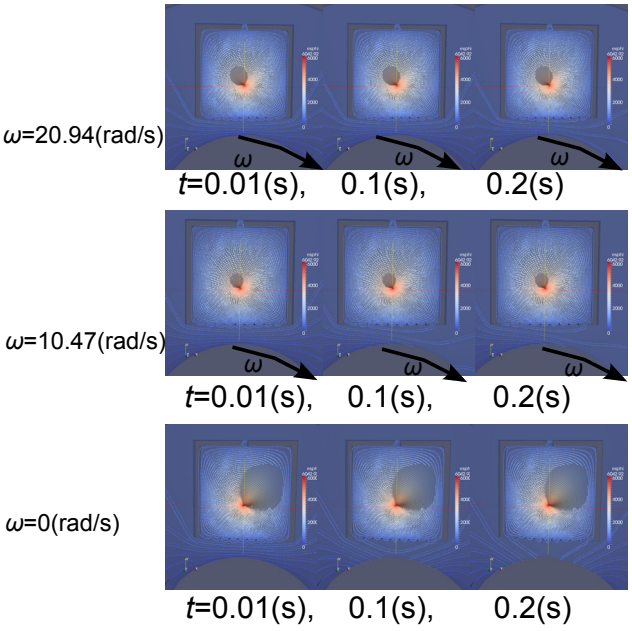

Figure 4. *Time dependence of electric potential contour with rotating ($\omega = 10.47, 20.94$(rad/s)) and non-rotating ($\omega = 0$(rad/s)) OPC. On top-middle-bottom raw of the figure, angular velocity is set $\omega = 20.94$(rad/s), $\omega = 10.47$(rad/s) and $\omega = 20.94$(rad/s) respectively. One left-center-right column of the figure, time is set $t = 0.01(s)$, $t = 0.1(s)$ and $t = 0.2(s)$. Contour lines are draw by every 100(V).*

In fig.(5), time dependencess of potential distributions on OPC with angular velocity $\omega = 0, 10.47, 20.94$(rad/s) are shown. In rotating OPC, as the peak position of the potential moves, the height grows with time and finally the distribution reached stationary state. We see that increasing the angular velocity ω results in the decrease of time to reach stationary states and the height of potential. The higher rotation means that staying time of OPC under scorotron and accumulated charge on OPC get smaller. Therefore, the time to reach stationary state decreases with angular velocity increasing. This results in the decrease of the potential on OPC. In non-rotating OPC, the peak position of the potential remains and the height and width grow with time. We see that the growth speed of the height of potential increases with corona current and depends on angle θ.

In fig.(6), time dependence of charge density are shown in the case with corona current $I/\ell = 1500(\mu A/m)$. We see that the charge density distribution changes with time and angular velocity. In non-rotating case ($\omega = 0$(rad/s)), the charge distribution

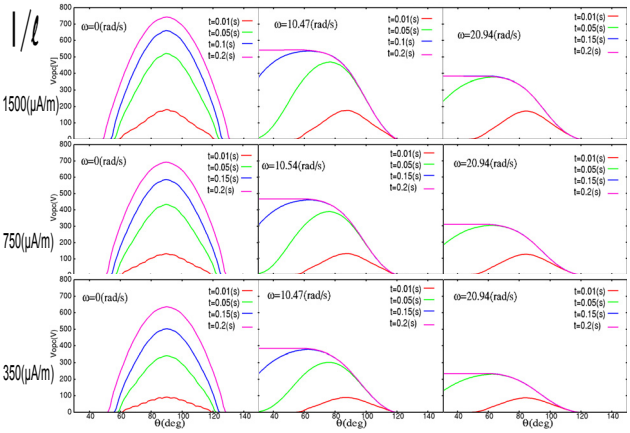

Figure 5. *Time dependence of electric potential on rotating and non-rotating OPC. On top-middle-bottom raw of the figure, corona current is set $I/\ell = 1500(\mu A/m)$, $I/\ell = 750(\mu A/m)$ and $I/\ell = 375(\mu A/m)$. One left-center-right column of the figure, angular velocity is set $\omega = 0$, $\omega = 10.47$(rad/s) and $\omega = 20.94$(rad/s).*

gets wider with time. This is due to charge accumulated on the top of OPC($=\theta = 90$(deg)). Then, the electric field between grid and top gets smaller(fig.(4)) and charge flows onto slightly different point on OPC. Continuing this cycle, the charge density distribution gets wider. In rotating case, the charge density is dense in upward of rotation and sparse in downward. As the point on OPC downward of rotation is already charged and upward is not, the electric field between grid and the point on OPC upward of rotation is stronger than that of downward (fig.(4)). This is the reason why the asymmetric charge density appears in rotating case.

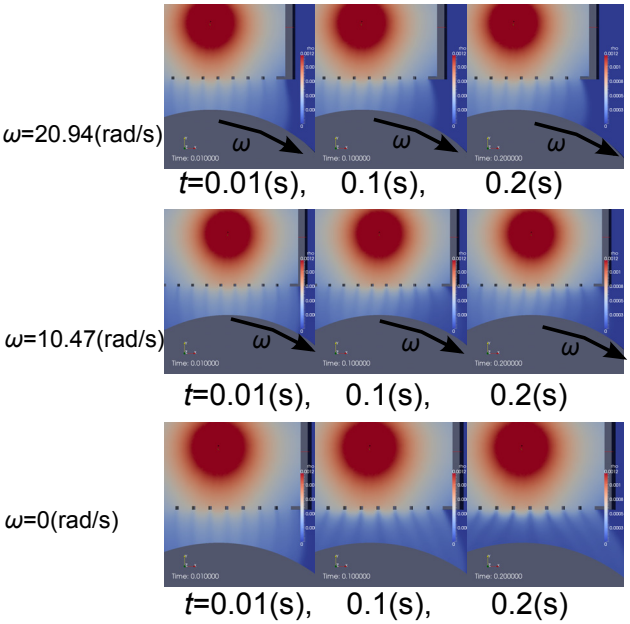

Figure 6. *Time dependence of charge density with rotating ($\omega = 10.47$(rad/s), 20.94(rad/s)) and non-rotating ($\omega = 0$(rad/s)) OPC. Angular velocity is set $\omega = 20.94$(rad/s) on the top, $\omega = 10.47$(rad/s) on the middle and $\omega = 20.94$(rad/s) on the bottom raw of the figure. Time is set $t = 0.01(s)$ on the left, $t = 0.1(s)$ on the middle and $t = 0.2(s)$ on the right column.*

In fig.(7), the time dependence of potential on non-rotating OPC $V_{opc}(\theta = 90(\mathrm{deg}))$ with corona current $I/\ell = 375, 750, 1500(\mu\mathrm{A/m})$ is shown. The authors show time dependence of $V_{opc}(\theta = 90(\mathrm{deg}))$ is well fitted with the function,

$$f(t) = V_0(1 - \exp(-t/\tau)/(1 - C\exp(-t/\tau)), \qquad (11)$$

where V_0, C, τ is potential in steady state, non-dimensional constant and time constant. This function $f(t)$ is similar to the model of Schaffert[7]. He modeled the potential on OPC globally (θ dependence of potential is not modeled). In the right side of fig.(7),

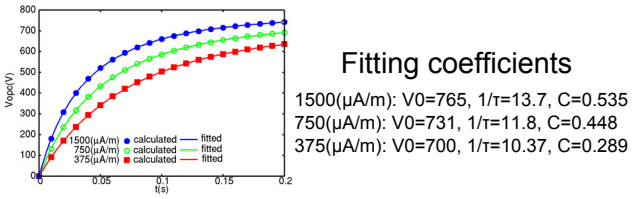

Figure 7. *Calculated time dependence of potential on non-rotating OPC $V_{opc}(\theta = 90(deg))$ and fitted curve(corona current $I/\ell = 375, 750, 1500(\mu A/m)$).*

the fitting parameters V_0, C, τ are shown. We take typical charging speed as $1/\tau$ and show the corona current dependence of it in fig.(8). We see the charging speed $1/\tau$ increase slowly with corona current of $I/\ell = 375(\mu A/m) - 1500(\mu\mathrm{A/m})$.

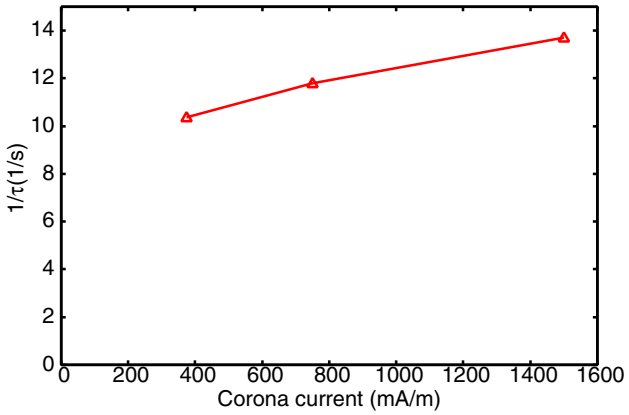

Figure 8. *Time constant τ of non-rotating OPC $V_{opc}(\theta = 90(deg))$.*

Conclusion

The authors have modeled the dynamics of charging OPC and ionic wind. Calculated results by the model well reproduced corona current dependence of the potential on rotating OPC and the velocity of ionic wind in steady state. The authors have shown the time dependence of potential around scorotron, on rotating/non-rotating OPC and charge density distribution. The authors have show charge density distribution between grid and OPC changes with time in rotating/non-rotating case. The authors have derived charging speed as inverse of time constant $1/\tau$ and its dependence of corona current.

Acknowledgments

The authors thank Mr. H. Fukuta and Mr. G. Kanazawa in Brother Industries for collaborating experiments. The authors also thank Mr. Y. Hata, Mr. Y. Maruyama, Mr. T. Hazeyama and Mr. M. Hanabusa in the same company for fruitful discussions.

References

[1] J. H. Chen, PhD Thesis, Univ. of Minnesota (2002).
[2] P. Zamankhan, G. Ahmadi and F. Fan, Imaging. Sci. and Technol., 50, 375 (2006).
[3] K. Mori, H. Okamoto and N. Hirooka, J. Imaging. Sci. and Technol., 48, 465 (2004).
[4] K. Mori, H. Okamoto, M. Shiraishi and A. Nishimura, J. Imaging. Sci. and Technol., 53, 040502 (2009).
[5] K. Mori, J. Imaging. Sci. and Technol., 54, 060501 (2010).
[6] K. Mori, Y. Nagamori, K. Otsuka, H. Okamoto, and T. Ito, J. Imaging. Soc. Japan. 49, 248 (2010) (In Japanese).
[7] R. M. Schaffert, *ELECTROPHOTOGRAPHY*, THE FOCAL PRESS, London and NewYork (1965).
[8] M. P. Sarma and W. Janischewskyj, PROC.IEE.116, pp.161(1969)
[9] F. W. Peek, *Dielectric Phenomena in High-Vlotage Engineering*, 3rd ed., McGraw-Hill, NewYork (1929).
[10] See http://www.openfoam.com/

Author Biography

Masato Kobayashi received his BS from Kyoto University (2000), his MS from the same University (2002) and his PhD degree in Nuclear Physics from the same University (2005). He joined Brother Industries, Ltd. in 2010. Since then, he has been working on the modeling physics in LBP. He has now been focused on charging process, ionic wind and plasma chemical reactions in positive DC corona discharges.